Properties of non-fcc hard-sphere solids predicted by density functional theory

James F. Lutsko*
Center for Nonlinear Phenomena and Complex Systems, Université Libre de Bruxelles, C.P. 231, Blvd. du Triomphe, 1050 Brussels, Belgium

(Received 21 April 2006; published 18 August 2006)

The free energies of the fcc, bcc, hcp, and simple cubic phases for hard spheres are calculated as a function of density using the fundamental measure theory models of Rosenfeld *et al.* [Phys. Rev. E **55**, 4245 (1997)], Tarazona [Phys. Rev. Lett. **84**, 694 (2001)], and Roth *et al.* [J. Phys.: Condens. Matter **14**, 12063 (2002)] in the Gaussian approximation. For the fcc phase, the present work confirms the vanishing of the Lindemann parameter (i.e., vanishing of the width of the Gaussians) near close packing for all three models and the results for the hcp phase are nearly identical. For the bcc phase and for packing fractions above $\eta \sim 0.56$, all three theories show multiple solid structures differing in the widths of the Gaussians. In all three cases, one of these structures shows the expected vanishing of the Lindemann parameter at close packing, but this physical structure is only thermodynamically favored over the unphysical structures in the Tarazona theory and even then, some unphysical behavior persists at lower densities. The simple cubic phase is stabilized in the model of Rosenfeld *et al.* for a range of densities and in the Tarazona model only very near close packing.

DOI: 10.1103/PhysRevE.74.021121 PACS number(s): 64.10.+h, 05.20.−y, 05.70.Ce

I. INTRODUCTION

The fundamental measure theory (FMT) approach to building approximate free energy density functionals has proven very successful in describing the properties of inhomogeneous hard-sphere fluids including the hard-sphere fcc solid [1–6]. The original form of FMT proposed by Rosenfeld [1,2] was based on a generalization of the ideas underlying scaled particle theory. The Rosenfeld functional gave a useful description of an inhomogeneous fluid but did not stabilize the fcc solid. One important formal property of the functional was that its second functional derivative with respect to the density reduced to the Percus-Yevik direct correlation function in the uniform liquid limit. Subsequent refinements were motivated in particular by the requirement that the free energy functional reduce to the known exact form when the density was restricted to zero- and one-dimensional systems [3]. The resulting theories, discussed in more detail below, retain all of the useful properties of the original Rosenfeld functional while also stabilizing the fcc solid and predicting the liquid-solid coexistence reasonably accurately [3–6]. The theories also give a good description of the mean-squared displacement of the atoms in the solid phase including the nontrivial prediction that the mean-squared displacement goes to zero as the density approaches close packing.

The purpose of this paper is to present the results of the application of the FMT to other crystalline structures of the hard-sphere solid. There are two good reasons for carrying out such a study. First, from a practical point of view, one would like to be able to use the FMT to study solid-solid phase transitions as well as a basis for the study, via thermodynamic perturbation theory, of non-fcc solids along the lines discussed in Refs. [7–10]. To do so with any confidence first requires that the predictions of the FMT for non-fcc hard-sphere solids be well understood. The second reason is that more loosely packed crystal structures may provide a more demanding test of the theory than does the fcc phase since the structure of the fcc phase is not that dissimilar to that of the liquid: other structures differ more from the liquid structure, e.g., in terms of the nearest-neighbor coordination. As shown below, this expectation is borne out and the predictions of the properties of the bcc phase in particular are not as satisfactory as for the fcc phase.

The remainder of this paper is organized as follows. Section II reviews the elements of density functional theory (DFT) and FMT and discusses the difference between the three FMTs considered in this work. The results of the calculations are presented in Sec. III where it is shown that the theories give very different results for different lattice structures. The final section summarizes the results of these calculations and discusses obstacles that prevent any simple modification of these theories to give a better description of the bcc phase.

II. FUNDAMENTAL MEASURE THEORY

As is usual in DFT, the Helmholtz free energy F is written as a sum of an ideal contribution F_{id} and an excess contribution F_{ex}. The former is given by

$$\beta F_{id}[\rho] = \int [\rho(\vec{r}) \ln \Lambda^3 \rho(\vec{r}) - \rho(\vec{r})] d\vec{r}, \tag{1}$$

where $\rho(\vec{r})$ is the local density, $N = \int \rho(\vec{r}) d\vec{r}$ is the total number of particles and $\beta = 1/k_B T$ is the inverse temperature. In the FMT approximation, the excess free energy functional is written in terms of a set of local functions,

$$\beta F_{ex}[\rho] = \int \sum_{i=1}^{3} \beta \phi_i(\{n_\alpha(\vec{r},[\rho])\}) d\vec{r} \tag{2}$$

which, as indicated, include a functional dependence on the density through a family of local functionals of the form

*Jlutsko@ulb.ac.be

$$n_\alpha(\vec{r},[\rho]) = \int w_\alpha(\vec{r}-\vec{r}')\rho(\vec{r}')d\vec{r}'. \tag{3}$$

The weights $w_\alpha(\vec{r})$ occurring in Eq. (3) are $\Theta(\frac{\sigma}{2}-r)$, $\delta(r-\frac{\sigma}{2})$, $\hat{r}\delta(r-\frac{\sigma}{2})$, and $\hat{r}\hat{r}\delta(r-\frac{\sigma}{2})$ yielding the local density functionals which will be denoted $\eta(\vec{r})$, $s(\vec{r})$, $\vec{v}(\vec{r})$, $\overleftrightarrow{T}(\vec{r})$, respectively. For a uniform liquid, in which $\rho(\vec{r})=\bar{\rho}$, one has, in three dimensions, that $\eta(\vec{r})=\frac{1}{6}\pi\sigma^3\bar{\rho}$ which is the usual definition of the packing fraction. The names of the other quantities are motivated by their scalar, vector, and tensor natures, respectively. The first two contributions to the excess free energy are

$$\beta\phi_1 = -\frac{1}{\pi\sigma^2}s(\vec{r})\ln[1-\eta(\vec{r})],$$

$$\beta\phi_2 = \frac{1}{2\pi\sigma}\frac{s(\vec{r})^2 - v^2(\vec{r})}{[1-\eta(\vec{r})]}. \tag{4}$$

These are the same as in the original Rosenfeld theory. The third function has been the focus of most efforts to refine the FMT and we write it in the form

$$\beta\phi_3 = \frac{1}{8\pi[1-\eta(\vec{r})]^2}f(\vec{r}), \tag{5}$$

where the only fundamental constraint on f is that $\lim_{\rho\to 0} f = 1$ [3]. Three proposals in the literature, aside from the original form $f=\frac{1}{3}s^3(\vec{r})$, which does not stabilize the bulk fcc solid, are

$$f_{RSLT} = \frac{1}{3}s^3(\vec{r})[1-\xi^2(\vec{r})]^3, \quad \xi^2 = \frac{v^2(\vec{r})}{s^2(\vec{r})},$$

$$f_T = \frac{3}{2}\{\vec{v}(\vec{r})\cdot\overleftrightarrow{T}(\vec{r})\cdot\vec{v}(\vec{r}) - s(\vec{r})v^2(\vec{r}) - Tr[\overleftrightarrow{T}^3(\vec{r})] + s(\vec{r})Tr[\overleftrightarrow{T}^2(\vec{r})]\},$$

$$f_E = \frac{2}{3}[1-\eta(\vec{r})]^2\left(\beta f_{ex}'[\eta(\vec{r})] + \ln[1-\eta(\vec{r})] - \frac{3\eta(\vec{r})}{1-\eta(\vec{r}),}\right)f_T, \tag{6}$$

where f_{RSLT} was proposed by Rosenfeld *et al.* [3] f_T is the tensor form proposed by Tarazona [4] and f_E is a heuristic modification of f_T that allows for the insertion of an empirical equation of state for the liquid, $\beta f_{ex}'(\eta)$. In the latter case, if the equation of state is chosen to be the Carnahan-Starling equation [11], the resulting free energy functional is the single-species version of the so-called "White Bear" functional of Roth *et al.* [6], which was also proposed by Tarazona [5]. The first and second forms are closely related. In fact, writing the tensor density as $\overleftrightarrow{T}(\vec{r}) = \overleftrightarrow{U}(\vec{r}) + \frac{1}{3}s(\vec{r})\overleftrightarrow{1}$, where $\overleftrightarrow{U}(\vec{r})$ is traceless, a natural approximation for the traceless part is to make it proportional to the only traceless tensor that can be formed from the other densities,

$$\overleftrightarrow{U}(\vec{r}) \approx A\frac{\vec{v}(\vec{r})\vec{v}(\vec{r}) - \frac{1}{3}\vec{v}^2(\vec{r})\overleftrightarrow{1}}{s(\vec{r})}, \tag{7}$$

where A is a constant and the denominator is needed so that $\overleftrightarrow{U}(\vec{r})$ scales linearly with the density in the sense that $\rho(\vec{r}) \to \lambda\rho(\vec{r})$ implies that $\overleftrightarrow{U}(\vec{r}) \to \lambda\overleftrightarrow{U}(\vec{r})$. Substituting this into f_T gives $f_T = \frac{1}{3}s^3(\vec{r})(1-3\xi^2+3A\xi^4-A^3\xi^6)$ which reduces to f_{RSLT} provided that one takes $A=1$. The choice $A=0$ corresponds to the original FMT theory of Rosenfeld. Note that one could also divide by $|\vec{v}(\vec{r})|$ rather than $s(\vec{r})$ in this ansatz, which is equivalent to the replacement $A \to A'\xi^{-1}(\vec{r})$ giving $f_T = \frac{1}{3}s^3(\vec{r})[1-3\xi^2+A'(3-A'^2)\xi^3]$. Taking $A'=1$ gives the "interpolation" form for ϕ_3 discussed in Ref. [3].

The calculations reported here were performed using the standard approximation of the density as a sum of Gaussians,

$$\rho(\vec{r}) = \sum_n f(\vec{r}-\vec{R}_n), \tag{8}$$

where $f(r) = x_0(\frac{\alpha}{\pi})^{3/2}\exp(-\alpha r^2)$. For a perfect lattice, one has occupancy $x_0=1$ whereas values $x_0<1$ characterize a solid with vacancies. The parameter α characterizes the width of the Gaussians and $\{\vec{R}_n\}$ is the set of lattice vectors of the desired crystal structure. The density can also be written in terms of components in reciprocal space as

$$\rho(\vec{r}) = \sum_n \exp(i\vec{K}_n\cdot\vec{r})\rho_n, \tag{9}$$

where $\{\vec{K}_n\}$ is the corresponding set of reciprocal lattice vectors and $\rho_n = x_0 N_{cell}\rho_{cell}\exp(-K_n^2/4\alpha)$ with N_{cell} being the number of lattice sites per unit cell and ρ_{cell} being the number of unit cells per unit volume. Thus $N_{cell}\rho_{cell}$ is just the number density of the perfect solid. From the fundamental theorems of DFT, the equilibrium values of the parameters x_0, ρ_{cell}, and α are those which minimize the grand potential, $\beta\Omega = \beta F_{id}[\rho] + \beta F_{ex}[\rho] - \beta\mu N$ for fixed chemical potential μ and volume V. The number of atoms is $N=\bar{\rho}V$ where the average density is $\bar{\rho} = \frac{1}{V}\int_V \rho(\vec{r})d\vec{r} = x_0 N_{cell}\rho_{cell}$.

The spatial integrals in Eqs. (1) and (2) were performed by sampling the arguments on a grid of points covering the standard unit cell. The primary consideration in fixing the number of points in the grid is that the spacing be sufficiently fine so as to be able to sample the width of the Gaussians, $(\Delta R)^2 = \frac{3}{2\alpha}$. In the calculations discussed below, the spacing of the points in each Cartesian direction was set to $dr = a/(2q)$ where a is the lattice parameter and q was initially set to 20 and then doubled until $dr/\Delta R < 0.5$. Increasing the number of points beyond this limit had no significant effect on the results. Note that in the Gaussian approximation and in the limit of $\alpha a^2 \gg 1$, the ideal contribution to the free energy approaches the asymptotic value

$$\beta f_{id} \to x_0\left[\frac{3}{2}\ln\left(\frac{x_0\alpha\sigma^2}{\pi}\right) - 2.5\right]. \tag{10}$$

This approximation was used for $\alpha a^2 > 200$. The plots of the free energy as a function of α presented below were all gen-

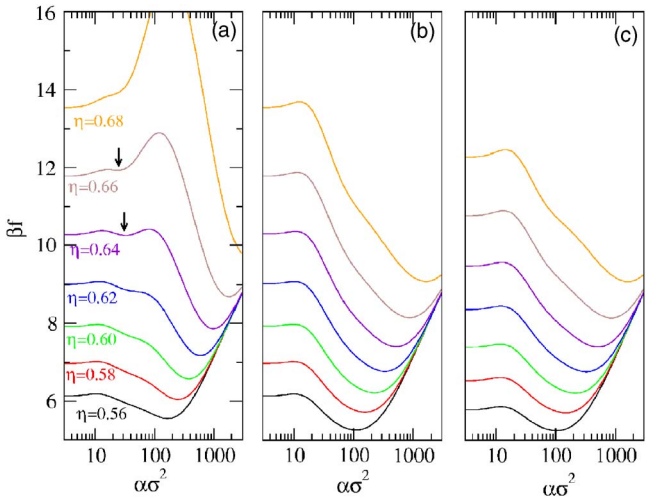

FIG. 1. (Color online) Dimensionless Helmholtz free energy per atom, $\beta f=\beta F/N$, as a function of α for the fcc hard-sphere solid as calculated using (a) the RSLT theory, (b) the Tarazona theory, and (c) the White Bear theory. From bottom to top, the curves are for $\bar{\eta}=0.56-0.68$ in steps of 0.02. The arrows indicate the positions of the secondary solid minima.

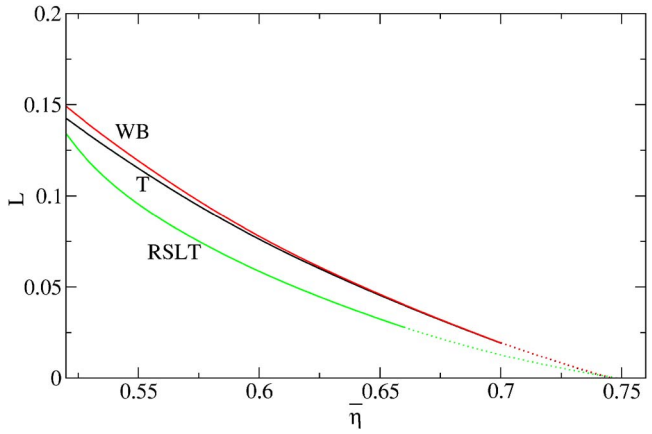

FIG. 2. (Color online) The Lindemann parameter for the fcc phase as a function of $\bar{\eta}$ as calculated using the RSLT theory (lower line), the Tarazona theory (middle curve labeled T) and the White Bear theory (upper curve labeled WB). Also shown as dotted lines are the quadratic interpolation of the curves to $L=0$ based on the data for $\bar{\eta}>0.60$.

erated based on sampling the free energy at intervals of $\delta\alpha\sigma^2=1$, 5, 10, 50, and 250 for $\alpha\sigma^2<20$, 200, 2000, 10 000, and 20 000, respectively. The free energy minima were determined using the the Simplex algorithm of Nelder and Mead, see, e.g., Ref. [12], as implemented in the Gnu Scientific Library [13], which was terminated when the simplex size was smaller than 10^{-4}.

III. RESULTS

A. fcc crystal

Figure 1 shows the free energies as a function of α for the fcc solid as calculated from the three theories for a variety of average packing fractions $\bar{\eta}=\frac{\pi}{6}\bar{\rho}\sigma^3$. These calculations are performed for $x_0=1$ which is known to be correct at the solid minimum [3] and which we have verified is very close to the free energy minimum at all values of α. All three theories show a minimum for all densities at $\alpha=0$ corresponding to the liquid phase. This is unphysical for the higher densities which are well above random close packing, $\bar{\eta}_{rcp}\sim 0.64$, and is a result of the use of the Percus-Yevik and Carnahan-Starling approximate equations of state which are only singular at $\bar{\eta}=1$. On the other hand, note the consistency in the location of the free energy minimum at finite α as well as of the value of the free energy at the minimum. While the location of the minimum in RSLT theory is somewhat higher than for the other two theories, the differences are not large. For all three theories, the location of the solid minimum increases rapidly with density which is a characteristic feature of the FMT [3,5]. The Tarazona and White Bear functionals differ primarily in the small-α region, due to the difference in the equations of state of the liquid, but at large α the differences are negligible. The main difference between the tensor theories and the RSLT theory is also in the small-α region where, for $\bar{\eta}>0.64$ the RSLT theory predicts much larger energy barriers between the liquid and solid minima than do the tensor theories. Note also that for a narrow range of densities, $0.61\lesssim\bar{\eta}\lesssim 0.63$, the RSLT theory actually shows *two* minima at nonzero values of α. This appears to be quite unphysical since all atoms are, by hypothesis, assumed to be identical and so it is hard to see how there could be two metastable states with the same density but different vibrational amplitudes.

The equilibrium free energy of the solid phase as a function of average density was determined by minimizing the free energy functional with respect to both α and the lattice parameter. From this, the densities of the coexisting liquid and solid as predicted by each theory were determined in the usual way by finding liquid and solid states with the same pressure and chemical potential. The RSLT theory gives the coexisting liquid and solid at packing fractions 0.491 and 0.534, respectively (compared to 0.491 and 0.540 reported in Ref. [3] and 0.491 and 0.534 reported in Ref. [14]), the Tarazona theory gives 0.466 and 0.516 (compared to 0.467 and 0.516 reported in Ref. [5]) and the White Bear theory 0.489 and 0.535 (compared to 0.489 and 0.536 reported in Ref. [5]). For comparison, the values from simulation are 0.492 and 0.545 [15]. The reason that the Tarazona theory gives relatively poor predictions for coexistence is, paradoxically, because it gives a rather good description of the solid while the liquid equation of state is still that of the Percus-Yevik theory which is inaccurate at the high densities that characterize coexistence [5]. This is one of the main motivations for introducing the empirical equation of state so that a free energy functional is obtained that yields accurate values over the entire range of structures.

The predicted Lindemann parameter, L which is the ratio of the root-mean-square displacement to the nearest neighbor distance, is shown in Fig. 2. For the fcc crystal, it decreases monotonically with increasing density and extrapolates to zero at a density near the fcc close-packing density of $\bar{\eta}_{\text{fcc-CP}}=\pi\sqrt{2}/6\sim 0.74$.

Similar calulations were performed for the hexagonal close-packed (hcp) phase. Since hcp only differs from fcc at

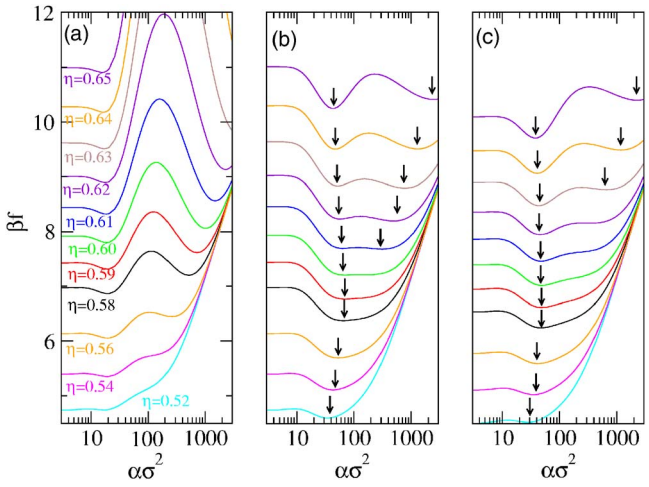

FIG. 3. (Color online) Same as 1 for the bcc phase. In (b) and (c), the arrows show the positions of the solid minima. From bottom to top, the curves are for $\bar{\eta}=0.52,0.54,0.56,0.58,0.59,0.60,0.61,0.62,0.63,0.64,0.65$.

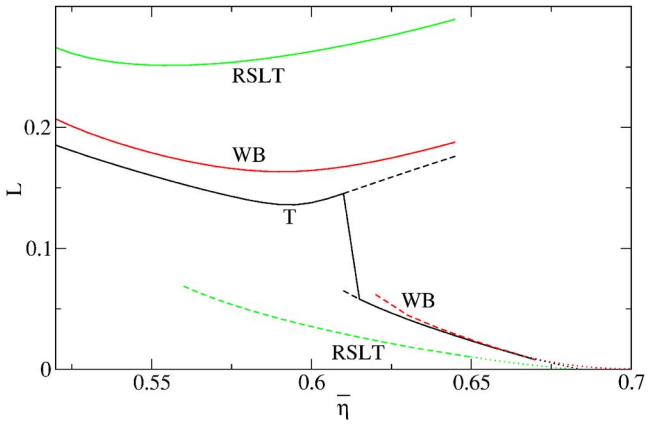

FIG. 4. (Color online) The Lindemann parameter for the bcc phase as a function of packing fraction $\bar{\eta}$ as calculated using the RSLT theory, the Tarazona theory (labeled T) and the White Bear theory (labeled WB). Both the low-α and high-α branches are shown with the stable branch being drawn with full lines and the unstable branch with dashed lines. Also shown as dotted lines are the quadratic interpolation of the curves to $L=0$ based on the data for $\bar{\eta}>0.60$.

the third nearest-neighbor shell, the free energies of the two phases are expected to be very similar. Nevertheless, the calculations are somewhat different as the fcc phase is a simple Bravais lattice whereas the hcp is a simple hexagonal lattice with a two-atom basis. As a result, it was found to be necessary to increase the minimum number of points used to integrate over the unit cell to 40 in order to obtain convergence in the case of the hcp structure. For a packing fraction of $\eta=0.545$, corresponding to the empirical melting point of the fcc lattice, the calculated difference in free energies per atom for the two lattice structures were of order $\beta f_{\rm fcc}-\beta f_{\rm hcp}\sim 10^{-6}$ using the tensor theories, and an order of magnitude smaller using the RLST theory. These results were independent of whether the lattice density was held fixed or relaxed. Neither increasing the number of points used in the integration nor reducing the tolerances used in the minimization routines affected the calculated free energy difference. Nevertheless, such small numerical differences could be due to subtle effects, such as round-off error, and the strongest conclusion should probably be that the free energies of the two phases are indistinguishable using FMT. At higher densities, the calculated free energy difference only decreased further, thus supporting the generality of this conclusion. In contrast, simulations have consistently indicated that at the melting point, the fcc phase is preferred with $\beta f_{\rm hcp}-\beta f_{\rm fcc}\sim 10^{-3}k_BT$ [16,17].

B. bcc crystal

Figure 3 shows the same calculations for the bcc solid. In this case, all three theories give multiple solid minima over some range of densities. For $\bar{\eta}\geqslant 0.56$, the RSLT theory gives two solid minima with the low-density minimum having lower free energy than the high-density minimum and thus being the preferred state. The Tarazona theory shows multiple minima for $\bar{\eta}\geqslant 0.61$ with energies that differ by less than 1%. In the range $0.61\leqslant\bar{\eta}\leqslant 0.63$ the low-α branch has slightly lower free energy while for $0.635\leqslant\bar{\eta}$ the high-α minimum is favored. The White Bear functional only develops a high-α minimum for $0.63\leqslant\bar{\eta}$ and in all cases the low-α minimum has lower free energy.

As seen in Fig. 4, the behavior of the Lindemann parameter for the bcc crystal is more complex than in the case of the fcc phase. All three theories give a "low-α" branch which is not monotonic: the Lindemann parameter decreases with increasing density at low densities, but then increases with increasing density at high densities. This behavior is similar to that of the effective-liquid-type DFTs [4,18] and is considered quite unphysical since, if the trend persisted up to close packing, it would imply that spheres are able to interpenetrate. Rather, one expects the mean-squared displacement to decrease uniformly with increasing density as in the case of the fcc crystal. All three FMTs also give a second, "high-α" branch which does behave physically at high densities and, in particular, the Lindemann parameter extrapolates to zero near the bcc close packing density of $\bar{\eta}_{\rm bcc-CP}=\pi\sqrt{3}/8\sim 0.68$. However, with the RSLT theory, up to $\bar{\eta}=0.625$, the well-behaved branch has higher free energy than does the unphysical branch. The Tarazona theory gives similar results except that the high-α minima are thermodynamically favored at high density so that, as noted by Tarazona [4,5], the prediction of the theory is that the Lindemann parameter appears to vanish near close packing, as it should. Nevertheless, the prediction of the theory is that the Lindemann parameter increases with increasing density at intermediate densities as well as giving a discontinuous jump in the Lindemann parameter for a packing fraction near 0.60, all of which seem somewhat unphysical. Finally, the White Bear theory also has a second branch but it only appears at very high densities and also has higher free energy than does the low-α branch. Comparison of Figs. 2(b) and 2(c) shows that the reason for the observed behavior is that the Carnahan-Starling equation of state used in the White Bear functional lowers the liquid free energy relative to the Percus-Yevik

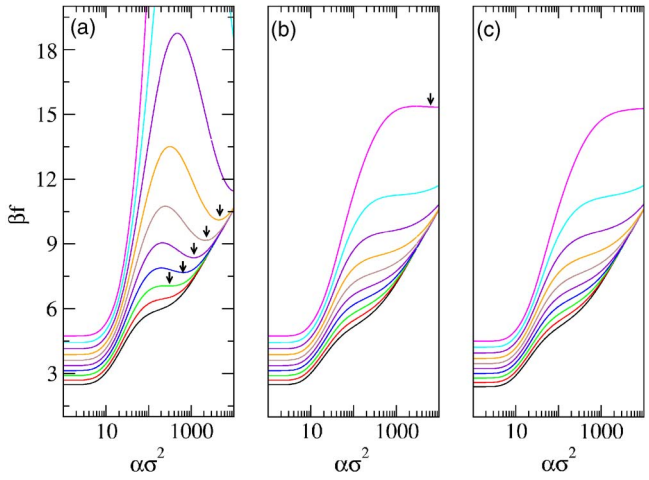

FIG. 5. (Color online) Same as Fig. 1 for the sc phase. From bottom to top, the curves are for $\bar{\eta}$ in the range [0.43,0.52] in steps of 0.01.

equation of state that comes out of the Tarazona theory. As α increases, the effect lessens until at high α the theories are almost identical. Thus the free energy of the low-α minimum is somewhat lower in the White Bear theory leading to its stability persisting even up to high densities.

C. sc phase

For a purely repulsive potential, the simple cubic phase is expected to be unstable with respect to shear. Nevertheless, there is no reason that DFT should not give a well-defined free energy for this structure since it should be metastable. Indeed, at least one of the effective-liquid theories, the Generalized Effective Liquid Approximation, does give a stable structure with small values of α [18].

Figure 5 shows the free energy curves calculated using the three theories. The results from the RSLT theory are much as expected: the simple cubic phase stabilizes at quite low densities, $\bar{\eta}\sim 0.45$, and the location of the free energy minimum increases with increasing density and appears to diverge as the simple cubic close packing, $\bar{\eta}_{\text{sc-cp}}=\pi/6\sim 0.524$ is approached. In this case, there is no indication of multiple minima. In contrast, the tensor theories show no sign of a $\alpha\neq 0$ minimum except at densities very close to close packing. Extending the calculations up to $\alpha\sigma^2=20\,000$, no minimum was found in the $\bar{\eta}=0.51$ curve using either of the tensor models while for $\bar{\eta}=0.52$ the Tarazona theory stablizes the solid at $\alpha\sigma^2\sim 11\,500$ and there is again no minimum using the White Bear (WB) theory.

D. Relative stability

The last question we adress is the relative stability of the various structures. Table I shows the minimum densities at which each structure becomes stable in the various FMT models. For the fcc and bcc structures, the RSLT and WB theories give quite similar results while the Tarazona theory generally stabilizes the solid at a lower density about 5% below the other theories. In all cases, the fcc phase is stable at lower densities than the bcc phase.

TABLE I. (Color online) The minimum packing fractions at which the various FMT models predict the different crystal structures become metastable and the approximate value of the Gaussian parameter α at this density.

Structure	Theory	$\bar{\eta}_{sol}$	$\alpha\sigma^2$
fcc	RSLT	0.49	27
	T	0.46	22
	WB	0.48	26
bcc	RSLT	0.51	14
	T	0.48	20
	WB	0.51	24
sc	RSLT	0.47	1150
sc	T	0.52	11 250
sc	WB		

The free energies as functions of the average density are shown in Fig. 6. In all models, the fcc phase has the lowest free energy of any solid phase at all densities. The free energy of the bcc phase is very close to that of the fcc at low densities and steadily diverges at increasing densities. The fcc phase has slightly higher free energy than the liquid at the lowest densities. The low-α branch of the bcc phase always has lower free energy than the liquid, although in the RSLT theory they are almost identical. In the RSLT, the simple cubic structure has much higher free energy than any other phase.

IV. CONCLUSIONS

In summary, the present calculations confirm the fact that the three FMT's discussed all give reasonable results for the

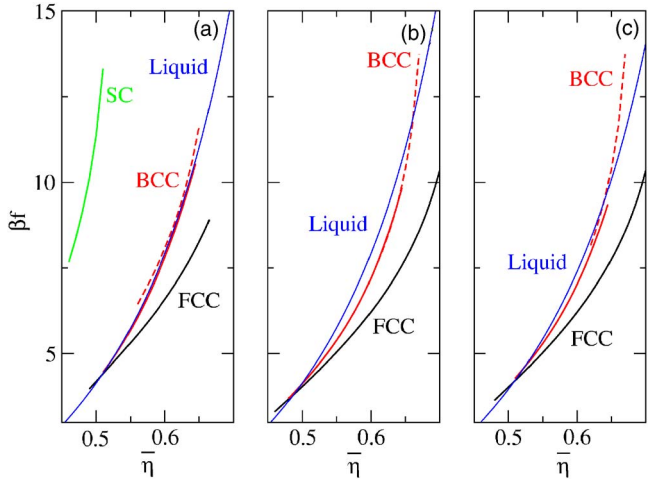

FIG. 6. (Color online) The free energy minima for the liquid phase and the various crystal structures as functions of the average packing fraction calculated using (a) the RSLT theory, (b) the Tarazona theory, and (c) the White Bear theory. The lowest curves are for the fcc structure, the intermediate curves are the low-α (full) and high-α (dashed) bcc branches and the light curve that spans the width of the figures are for the liquid phase. In (a), the upper curve is for the simple cubic structure.

fcc phase at all densities up to fcc close packing with the only exception being the appearance of a spurious low-α minimum at high densities in the RSLT theory. None of the theories were able to meaningfully differentiate between the hcp and fcc phases. On the other hand, when applied to the bcc phase, these results indicate several unphysical properties of the fundamental measure theory functionals which must be carefully considered when using them, e.g., as the basis for thermodynamic perturbation theory. All of the theories appear to give reasonable results at moderate densities, say up to $\bar{\eta}\sim 0.56$. However, the simplest model, the RSLT, gives multiple solid minima for all packing fractions in the bcc phase above about 0.56. The Tensor theories do not give multiple minima for the fcc phase but they do for the bcc phase. As the density increases, the stable minima in the Tarazona theory switches from the unphysical branch to the physically well-behaved branch whereas the White Bear theory always picks out the unphysical branch. Only the RSLT and Tarazona theories stablize the simple cubic phase, at least for $\alpha\sigma^2 < 20\,000$, but the Lindemann parameter is, in this case, well-behaved and there are no spurious minima. Unfortunately for the goal of choosing a single theory to describe both the liquid and all solid phases, the RSLT and WB theories give poor results for the bcc phase Lindemann parameter while the Tarazona theory gives the worst quantitative description of fcc-liquid coexistence.

It is interesting to speculate on the resolution of the common deficiencies in these theories. It seems reasonable to attribute the unphysical behavior at high densities, which is manifested by the fact that the unphysical low-α minimum is favored, to a poor description of the liquid phase: the free energy of the liquid must clearly diverge at high densities and in fact it has long been debated whether the hard-sphere liquid-phase equation of state possesses a singularity at high densities [19]—at, e.g., random close packing [20] or fcc close packing [21]. If the free energy of the liquid did indeed diverge at random close packing, then the curves shown in Figs. 1 and 3 would be deformed with the low-α free energies "pulled up." This could conceivable eliminate altogether the low-α minima and thus give a reasonable picture of the bcc phase. However, as appealing as this scenario is, it cannot be implemented naively using Eq. (6) to give the equivalent of the "White Bear" improvement to the Tarazona theory. This is because Eq. (6) requires that the equation of state be evaluated at the local packing fraction $\bar{\eta}(\vec{r})$ and for the solid phase there are always points at which $\eta(\vec{r})$ is very nearly equal to 1 unless α is very small. [In particular, it is easy to see that $\lim_{\alpha\to\infty}\eta(\vec{0})=1$.] Thus simply inserting an equation of state with a divergence for $\bar{\eta}<1$ is not an option since this will lead to divergent free energies in the solid phase, even for the already well-described fcc phase. A further problem with this type of development is that larger packing fractions can also occur in the case of mixtures of different sized spheres so that any simple divergence at large packing fractions could be problematic in this case as well.

One approximation not tested here is the use of the Gaussian profile for the densities. Tarazona has performed calculations using more general parametrizations of the density and he reports that the generalization beyond the Gaussian is of negligble importance for the equation of state [4]. Groh and Mulder have also supplied evidence for the fcc phase that the Gaussian approximation is quite accurate, especially near the peaks of the density distribution [22]. This suggests that the effects reported here are not due to the Gaussian approximation but definitive proof will require further calculations using non-Gaussian profiles.

In summary, the fundamental measure theories work well for the fcc (and hcp) phase at all densities while for the bcc phase, the FMTs are best applied to the solid phase for densities near liquid-solid coexistence. While they can in principle be used to model the bcc phase at higher densities, and while they do show some desirable features at high density like the vanishing of the Lindemann parameter at close packing, they also suffer from the same problem that plagued earlier DFT models: namely, the unphysical behavior of the Lindemann parameter for the bcc phase at intermediate densities. On the other hand, the sc phase is well modeled, at least using the RSLT theory, perhaps because it only exists at relatively low densities.

ACKNOWLEDGMENTS

I am grateful to Marc Baus and Xeyeu Song for several stimulating discussions on this topic. This work was supported in part by the European Space Agency/PRODEX under Contract No. C90238.

[1] Y. Rosenfeld, Phys. Rev. Lett. **63**, 980 (1989).
[2] Y. Rosenfeld, D. Levesque, and J.-J. Weis, J. Chem. Phys. **92**, 6818 (1990).
[3] Y. Rosenfeld, M. Schmidt, H. Löwen, and P. Tarazona, Phys. Rev. E **55**, 4245 (1997).
[4] P. Tarazona, Phys. Rev. Lett. **84**, 694 (2000).
[5] P. Tarazona, Physica A **306**, 243 (2002).
[6] R. Roth, R. Evans, A. Lang, and G. Kahl, J. Phys.: Condens. Matter **14**, 12063 (2002).
[7] W. A. Curtin and N. W. Ashcroft, Phys. Rev. Lett. **56**, 2775 (1986).
[8] J. F. Lutsko and M. Baus, J. Phys.: Condens. Matter **3**, 6547 (1991).
[9] C. F. Tejero, J. F. Lutsko, J. L. Colot, and M. Baus, Phys. Rev. A **46**, 3373 (1992).
[10] V. B. Warshavsky and X. Song, Phys. Rev. E **69**, 061113 (2004).
[11] J.-P. Hansen and I. McDonald, *Theory of Simple Liquids* (Academic Press, San Diego, 1986).
[12] W. H. Press, S. A. Teukolsky, W. T. Vetterling, and B. P. Flannery, *Numerical Recipes in C* (Claredon Press, Oxford, 1993).
[13] The Gnu Scientific Library, http://sources.redhat.com/gsl

[14] V. B. Warshavsky and X. Song, Phys. Rev. E **73**, 031110 (2006).
[15] W. G. Hoover and F. H. Ree, J. Chem. Phys. **49**, 3609 (1968).
[16] S.-C. Mau and D. A. Huse, Phys. Rev. E **59**, 4396 (1999).
[17] A. D. Bruce, N. B. Wilding, and G. J. Ackland, Phys. Rev. Lett. **79**, 3002 (1997).
[18] J. F. Lutsko and M. Baus, Phys. Rev. A **41**, 6647 (1990).
[19] N. Clisby and B. M. McCoy, J. Stat. Phys. **122**, 15 (2006).
[20] D. Ma and G. Ahmadi, J. Chem. Phys. **84**, 3449 (1986).
[21] I. C. Sanchez, J. Chem. Phys. **101**, 7003 (1994).
[22] B. Groh and B. Mulder, Phys. Rev. E **61**, 3811 (2000).